Cross sections for excitation of the $b\,^3\Sigma_u^+$, $a\,^3\Sigma_g^+$, and $c\,^3\Pi_u$ states of H_2 by low-energy electrons

M. A. P. Lima,* T. L. Gibson,† and V. McKoy

*Arthur Amos Noyes Laboratory of Chemical Physics, California Institute of Technology,
Pasadena, California 91125*

W. M. Huo

National Aeronautics and Space Administration, Ames Research Center, MS 230-3, Moffett Field, California 94035

We used a multichannel extension of the Schwinger variational principle [K. Takatsuka and V. McKoy, Phys. Rev. A **24**, 2473 (1981)] to study the cross sections for excitation of the $X\,^1\Sigma_g^+ \to b\,^3\Sigma_u^+$, $a\,^3\Sigma_g^+$, and $c\,^3\Pi_u$ transitions in H_2 by low-energy electrons. These cross sections were obtained with two open channels for each transition and for energies near threshold to 30 eV. The results for the $b\,^3\Sigma_u^+$ and $a\,^3\Sigma_g^+$ states agree quite well with available experimental data. However, the cross sections for excitation of the $c\,^3\Pi_u$ state differ significantly from the measured values at the two energies, 20 and 30 eV, where data are available.

I. INTRODUCTION

Cross sections for electronic excitation of molecules by low-energy electrons play an important role in the modeling of swarm and plasma etching systems,[1] discharge devices, gas lasers,[2] flow fields around space vehicles,[3] and planetary atmospheres. Electronic excitation of adsorbed molecules by low-energy electrons is furthermore a potentially important probe of adsorbate-substrate structure in surface science.[4] The available experimental data on these cross sections is fragmentary[5] and, in some cases, show major inconsistencies. Most theoretical studies of electronic excitation of molecules by low-energy electrons to date have also been carried out using low-order theories such as the Born and Ochkur-Rudge approximations,[6,7] the impact-parameter method,[8] and distorted-wave theories.[9–11] Though such theories can be computationally easy to apply and can provide useful results in some applications, they cannot be expected to yield consistently reliable differential and integral cross sections at low and intermediate collision energies. Recently, however, the Schwinger variational, linear algebraic, and R-matrix methods[12] which had previously been widely applied to elastic electron-molecule collisions were extended, where necessary, and applied to electronic excitation of H_2^+,[13–15] H_2,[16–18] and O_2 (Ref. 19) by low-energy electrons. In these studies of H_2,[16–18] our excitation cross sections for the $X\,^1\Sigma_g^+ \to b\,^3\Sigma_u^+$ transition were obtained using a multichannel extension of the Schwinger variational method which was formulated so as to be specifically applicable to electron-molecule collisions.[20,21] The results of these two-channel calculations[16] were in good agreement with those obtained by the linear algebraic[17] and R-matrix methods[18] and with available experimental data.[22–24] Furthermore, the studies of Schneider and Collins explicitly showed that inclusion of correlation terms in the expansion of the scattering wave function so as to relax the orthogonality usually imposed on bound and scattering orbitals affected the cross sections

substantially.[17] Note that earlier Schwinger two-channel calculations,[25] in which such correlation terms were included, erroneously gave smaller cross sections than the results shown in Ref. 16 due to an error in the computer codes.

In this paper we present the results of applications of our Schwinger multichannel formulation to low-energy electron-impact excitation of the $a\,^3\Sigma_g^+$, $c\,^3\Pi_u$, and $b\,^3\Sigma_u^+$ states of H_2. In these two-channel studies both differential and integral cross sections have been obtained for collision energies from near threshold to 30 eV. For the $X\,^1\Sigma_g^+ \to b\,^3\Sigma_u^+$ excitation, in addition to the differential cross sections at two energies discussed in an earlier communication,[16] here we report cross sections at several other energies along with some intermediate results which should provide useful insight into the nature of these cross sections. Our results for excitation of the $b\,^3\Sigma_u^+$ and $a\,^3\Sigma_g^+$ states agree quite well with available experimental data. For the $c\,^3\Pi_u$ state, however, significant differences are seen between our two-state results and the limited experimental data for this transition. While we are currently examining multichannel effects as a possible cause of our discrepancies with experiment, these two-state results are of interest by themselves. Together with an earlier study of the $B\,^1\Sigma_u^+$ state of H_2,[26] they represent an important step forward in studies of low-energy electron-impact excitation of a molecule at the two-state level.

The outline of the paper is as follows. In Sec. II we give a brief discussion of the multichannel Schwinger variational formulation used in these studies. We then discuss the relevant computational details and present both differential and integral cross sections for excitation of the $b\,^3\Sigma_u^+$, $a\,^3\Sigma_g^+$, and $c\,^3\Pi_u$ states at several energies. Finally, these results are compared with those obtained previously by the close-coupling and more approximate approaches, e.g., the distorted-wave and Born-Rudge methods, and with available measurements of these cross sections.

II. MULTICHANNEL EQUATIONS

The Schwinger multichannel formulation used here has been discussed in detail elsewhere[20,21,27] and only a brief outline essential to highlighting some relevant features of the method wil be given here. The Hamiltonian for the collision can be written as

$$H = (H_N + T_{N+1} + V) = H_0 + V , \tag{1}$$

where H_N is the target Hamiltonian, T_{N+1} is the kinetic energy operator for the incident electron, and V is the interaction between the incident electron and the nuclei and electrons of the target. The Lippmann-Schwinger equation for the scattering wave function $\Psi_m^{(+)}$ is

$$\Psi_m^{(+)} = S_m + G_0^{(+)} V \Psi_m^{(+)} . \tag{2}$$

In Eq. (2) $G_0^{(+)}$ is the Green's function associated with $E - H_0$ and S_m is an eigenfunction of H_0, i.e.,

$$S_m = \Phi_m(1,2,\ldots,N)e^{i\mathbf{k}_m \cdot \mathbf{r}_{N+1}} . \tag{3}$$

Here Φ_m is a target eigenfunction of H_N with energy E_m and E is the total collision energy. For collisions of identical particles Eq. (2) has the drawback of requiring that the continuum states of the target molecule be included in $G_0^{(+)}$. To develop an alternative multichannel formulation, we proceeded as follows.[20,21,27] A projection operator P, defined by the open channels of the target,

$$P = \sum_l^{\text{open}} |\Phi_l(1,2,\ldots,N)\rangle\langle\Phi_l(1,2,\ldots,N)| , \tag{4}$$

is projected onto Eq. (2) to yield

$$P\Psi_m^{(+)} = S_m + G_p^{(+)} V \Psi_m^{(+)} , \tag{5}$$

where

$$G_P^{(+)} = \sum_l^{\text{open}} |\Phi_l\rangle g_l^{(+)}(\mathbf{r}_{N+1}, \mathbf{r}'_{N+1})\langle\Phi_l| \tag{6}$$

and $g_l^{(+)}$ denotes the Green's function for T_{N+1} at energy $E - E_l$. To recover the closed-channel component of $\Psi_m^{(+)}$ and hence to obtain a complete equation for the scattering wave function we write the Schrödinger equation in the form

$$(E - H)\Psi_m^{(+)} = \hat{H}\Psi_m^{(+)} = \hat{H}[aP\Psi_m^{(+)} + (1 - aP)\Psi_m^{(+)}] = 0 , \tag{7}$$

where a is an arbitrary parameter. Using Eq. (5) we can write Eq. (7) as

$$\hat{H}[a(S_m + G_p^{(+)} V \Psi_m^{(+)}) + (1 - aP)\Psi_m^{(+)}] = 0 . \tag{8}$$

Rearrangement of Eq. (8) gives a multichannel equation for $\Psi_m^{(+)}$, i.e.,

$$A\Psi_m^{(+)} = VS_m , \tag{9}$$

where

$$A^{(+)} = \tfrac{1}{2}(PV + VP) - VG_p^{(+)}V$$

$$+ \frac{1}{a}[\hat{H} - (a/2)(\hat{H}P + P\hat{H})] . \tag{10}$$

We have shown previously that the variational stability of functionals for the scattering amplitude based on Eq. (9) requires that the parameter a be chosen equal to $N + 1$.[20,27] Using Eq. (9) with this choice of a, a variational expression for the scattering amplitude can be written in bilinear form

$$f_{m,n} = -\frac{1}{2\pi}(\langle S_m | V | \Psi_n^{(+)}\rangle + \langle \Psi_m^{(-)} | V | S_n \rangle$$

$$- \langle \Psi_m^{(-)} | A^{(+)} | \Psi_n^{(+)}\rangle) . \tag{11}$$

Expansion of trial scattering wave functions for $\Psi_n^{(+)}$ and $\Psi_m^{(-)}$ in Eq. (11) in the form $\sum_i c_i^{(\mp)}\chi_i$ and stationarity of $\tilde{f}_{m,n}$ with respect to the coefficients $c_i^{(\mp)}$ lead straightforwardly to our working equation.

$$\tilde{f}_{m,n} = -\frac{1}{2\pi}\sum_{i,j}\langle S_m | V | \chi_i\rangle(A^{-1})_{ij}\langle\chi_j | A | S_n\rangle , \tag{12}$$

where $A_{ij} = \langle\chi_i | A^{(+)} | \chi_j\rangle$.

Equation (12) is the multichannel variational form used in our present studies of electron-impact excitation of H_2. Some important features of this method are as follows. An expansion of the trial scattering wave function in a discrete basis is possible. Furthermore, if the one-electron functions appearing in the $(N+1)$-electron determinants χ_i are chosen to be Cartesian Gaussian functions, all matrix elements arising in Eq. (12), except those of $VG_p^{(+)}V$, can be evaluated analytically for a general molecular target.[28] The matrix elements associated with $VG_p^{(+)}V$ can also be obtained analytically if a large quadrature basis of Cartesian Gaussian functions is inserted around $G_p^{(+)}$. We use this technique to obtain the principal-value contribution to the $VG_p^{(+)}V$ matrix elements but we evaluate the on-shell contribution via insertion of a complete set of plane waves around $G_p^{(+)}$. This procedure results in an S matrix that is very nearly unitary without resorting to large Gaussian insertion basis sets.[29]

Finally, Eq. (12) provides an analytical approximation to the body-frame fixed-nuclei scattering amplitude for molecules of arbitrary geometry. Our procedure for obtaining the physical scattering cross sections has been discussed elsewhere.[25] In the present calculation, we obtain the full scattering amplitude in the body frame $f(\mathbf{k}_f, \mathbf{k}_i)$ for 64 orientations of each vector $\mathbf{k}_i$ and $\mathbf{k}_f$. These orientations are chosen via an eight-point Gauss-Legendre quadrature for integration over $\Theta(0 \to \Pi)$ and likewise for $\phi(0 \to \Pi)$. From the results in this hemisphere, those in the opposite hemisphere can be obtained straightforwardly via the relationship $\langle S_{-\mathbf{k}_f} | V | \chi_i\rangle = \langle S_{\mathbf{k}_f} | V | \chi_i\rangle^*$. Molecular symmetry will generally reduce the number of orientations at which these amplitudes must be calculated. By Gaussian-Legendre quadrature we then generate the partial-wave representation of this body-frame scattering amplitude needed for the transformation to the laboratory frame.

III. PROCEDURES AND RESULTS

Our calculations have been carried out within the framework of the fixed-nuclei and Franck-Condon approximations. The physical cross sections were obtained by averaging the fixed-nuclei results over all molecular orientations. All the calculations used the equilibrium distance of the ground state, $1.40a_0$, and the theoretical vertical excitation energies. The self-consistent-field (SCF) wave function of the $X\,^1\Sigma_g^+(1\sigma_g^2)$ state was calculated using an uncontracted $6s\,6p$ Cartesian Gaussian basis on the nuclei and a $4s\,4p$ basis at the molecular center, as shown in Table I. The SCF energy is -1.133 a.u. The same basis was used to represent the $b\,^3\Sigma_u^+(1\sigma_g 1\sigma_u)$ and $a\,^3\Sigma_g^+(1\sigma_g 2\sigma_g)$ states. For the $X\,^1\Sigma_g \rightarrow c\,^3\Pi_u$ transition this basis is supplemented with $6d_{xy}$ functions on each nucleus, primarily to provide a better description of the $^2\Delta$ component of the wave function. The excited-state wave functions were determined using the frozen-core approximation and diagonalizing the V_{N-1} potential of the frozen core to determine the excited orbitals ($1\sigma_u$, $2\sigma_g$, and $1\pi_u$). The vertical excitation energies determined in this manner are 9.975, 12.036, and 12.306 eV for the $b\,^3\Sigma_u^+$, $a\,^3\Sigma_g^+$, and $c\,^3\Pi_u$ transitions, respectively. These values can be compared with the experimental "vertical" excitation energies of 10.35, 12.28, and 12.60 eV from the $v=0$ vibrational level of the ground state for these same transitions. The zero-point vibrational energy is taken as 0.27 eV here. The entire set of eigenfunctions of the V_{N-1} potential, i.e., the improved virtual orbitals,[30] is used to expand the $(N+1)$-electron wave functions and in the insertion quadratures for the $VG_p^{(+)}V$ terms. For excitation of the $b\,^3\Sigma_u^+$ and $a\,^3\Sigma_g^+$ states, the expansion of the scattering wave function $\Psi^{(+)}$ consists of all possible $(N+1)$-electron Slater determinants which are associated with either the ground or excited state target wave functions and have $^2\Sigma_g^+$, $^2\Sigma_u^+$, $^2\Pi_u$, or $^2\Pi_g$ overall symmetries. For the $c\,^3\Pi_u$ excitation, $^2\Delta_g$ and $^2\Delta_u$ symmetries are also included.

As noted above, the trial scattering wave functions used in these calculations are expanded in $(N+1)$-Slater determinants. So as not to impose any unphysical orthogonality condition between our single-particle scattering function and the bound target orbitals, this expansion in-

cludes the so-called correlation terms, i.e., $1\sigma_g^2 1\sigma_u$ and $1\sigma_g 1\sigma_u^2$ terms for the $X\,^1\Sigma_g^+(1\sigma_g^2) \rightarrow b\,^3\Sigma_u^+(1\sigma_g 1\sigma_u)$ transition, $1\sigma_g^2 2\sigma_g$ and $1\sigma_g 2\sigma_g^2$ for the $a\,^3\Sigma_g^+(1\sigma_g \sigma_g)$ excitation, and $1\sigma_g^2 1\pi_u$ and $1\sigma_g 1\pi_u^2$ for the $c\,^3\Pi_u$ excitation.

Figures 1–6 show our calculated differential excitation cross sections for the $X\,^1\Sigma_g^+ \rightarrow b\,^3\Sigma_u^+$ transition at col-

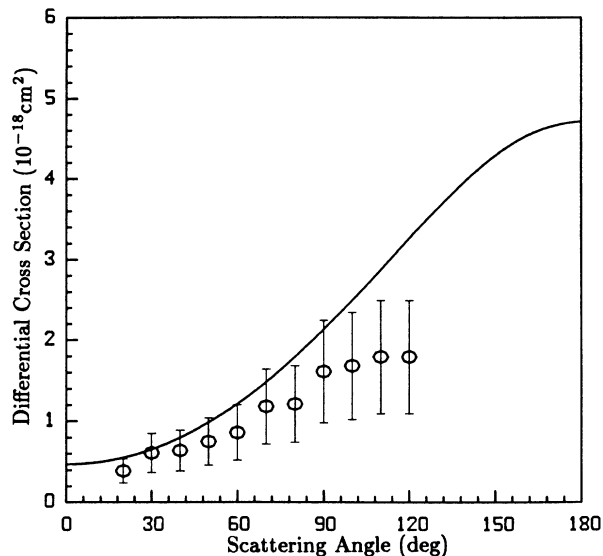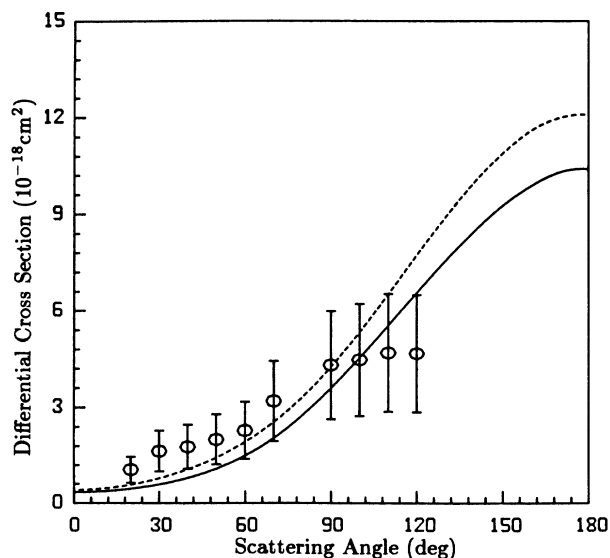FIG. 1. Differential cross sections for excitation of the $b\,^3\Sigma_u^+$ state at 10.5 eV: ———, present results; O, measured values of Ref. 22.

FIG. 2. Differential cross sections for excitation of the $b\,^3\Sigma_u^+$ state at 12 eV: ———, present results; — — —, distorted-wave results (Ref. 10); O, measured values of Ref. 22.

TABLE I. Cartesian Gaussian basis. $\chi = N_{lmn}(x - A_x)^l(y - A_y)^m(z - A_z)^n \exp(-\alpha\,|\,r - A\,|^2)$.

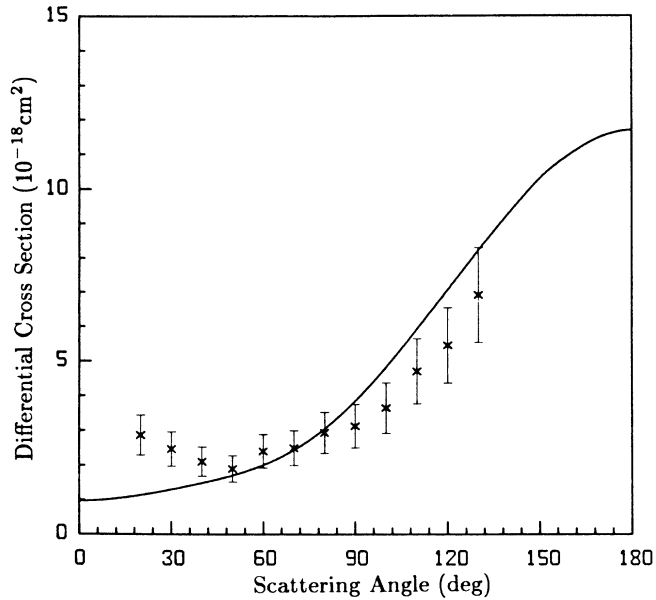| Center and type	Exponent
H, $6s$	48.4479, 7.283 46, 1.651 39, 0.462 447, 0.145 885, 0.07
H, $6p$	4.5, 1.5, 0.5, 0.25, 0.125, 0.031 25
CM, $4s^{\text{a}}$	0.25, 0.05, 0.01, 0.002
CM, $4p$	0.8, 0.2, 0.0625, 0.007 81
H, $6d_{xy}$	4.5, 1.5, 0.5, 0.25, 0.125, 0.031 25

[a]Center of molecule.

FIG. 3. Differential cross sections for excitation of the $b\ ^3\Sigma_u^+$ state at 13 eV: ——, present results; $\times$, measured values of Ref. 23.

FIG. 5. Differential cross sections for excitation of the $b\ ^3\Sigma_u^+$ state at 20 eV: ——, present results; – – –, distorted-wave results (Ref. 10); $\times$ and $\blacktriangle$, measured values of Refs. 23 and 24, respectively.

lision energies of 10.5, 12, 13, 15, 20, and 30 eV along with available experimental data.[22–24] The differential cross sections at nine energies are also given in Table II. The results at 12 and 20 eV have already been presented in a previous communication.[16] The agreement between the calculated and measured differential cross sections at
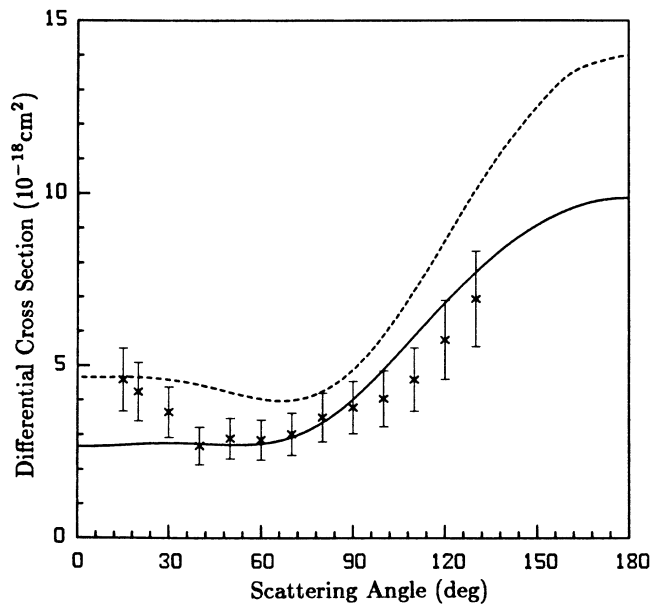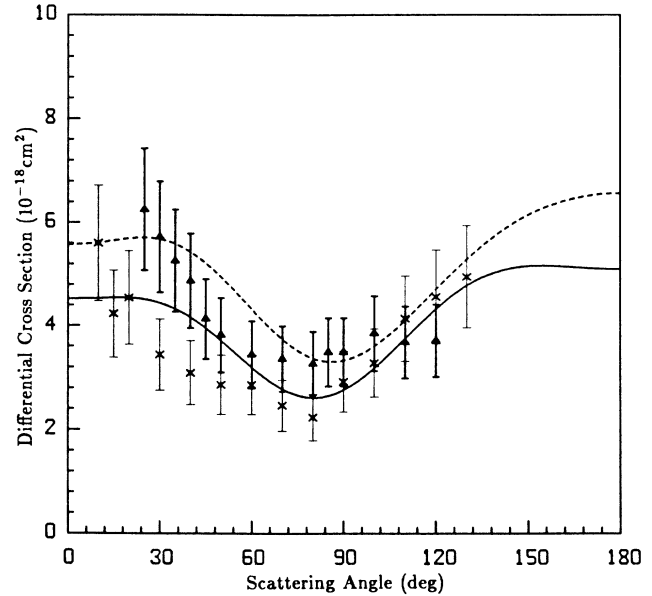
these six energies is, in general, quite good. The experimental data of Nishimura and Danjo[23] at 13 and 15 eV show some forward peaking which is not seen in the calculated results.

In Fig. 7 we show our integral cross sections for excitation of the $b\ ^3\Sigma_u^+$ state along with the experimental data
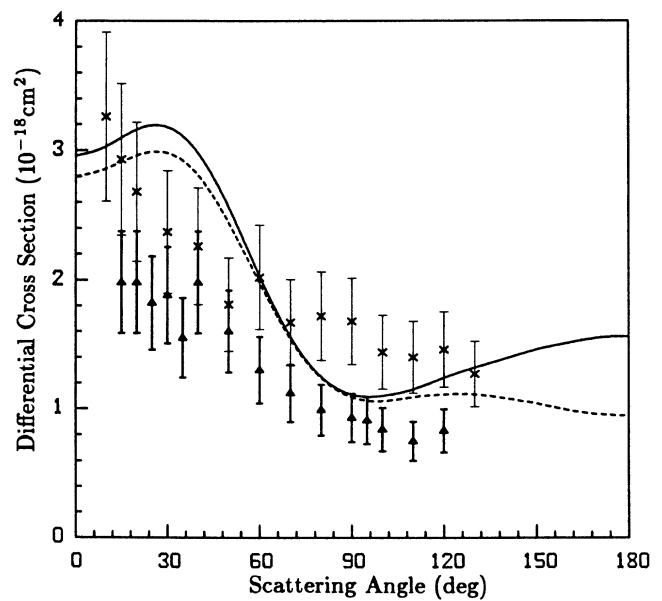

FIG. 4. Differential cross sections for excitation of the $b\ ^3\Sigma_u^+$ state at 15 eV: ——, present results; – – –, distorted-wave results (Ref. 10); $\times$, measured values of Ref. 23.

FIG. 6. Differential cross sections for excitation of the $b\ ^3\Sigma_u^+$ state at 30 eV: ——, present results; – – –, distorted-wave results (Ref. 10); $\times$ and $\blacktriangle$, measured values of Refs. 23 and 24, respectively.

TABLE II. Differential cross sections for the $X\,^1\Sigma_g^+ \to b\,^3\Sigma_u^+$ excitation $(10^{-18}\,cm^2/\,sr)$. The threshold energy is 9.975 eV.

Scattering angle (deg.)	Collision energy (eV)								
	10.5	11	12	13	15	18	20	25	30
0	0.470	0.199	0.344	0.961	2.66	4.20	4.52	3.94	2.96
10	0.491	0.231	0.370	1.01	2.68	4.20	4.53	3.97	3.03
20	0.551	0.325	0.451	1.13	2.73	4.19	4.54	4.01	3.16
30	0.653	0.482	0.587	1.29	2.76	4.09	4.44	3.94	3.18
40	0.798	0.705	0.789	1.48	2.74	3.85	4.16	3.67	2.98
50	0.985	0.997	1.08	1.70	2.71	3.49	3.71	3.19	2.56
60	1.21	1.37	1.49	2.00	2.74	3.13	3.20	2.62	2.03
70	1.48	1.82	2.04	2.43	2.93	2.91	2.78	2.12	1.56
80	1.79	2.35	2.75	3.04	3.35	2.96	2.61	1.82	1.25
90	2.13	2.96	3.59	3.84	4.02	3.32	2.76	1.76	1.11
100	2.49	3.63	4.53	4.82	4.89	3.95	3.18	1.92	1.10
110	2.87	4.35	5.54	5.92	5.86	4.71	3.75	2.19	1.15
120	3.26	5.08	6.56	7.07	6.83	5.46	4.32	2.49	1.24
130	3.63	5.82	7.55	8.22	7.72	6.06	4.78	2.72	1.32
140	3.98	6.50	8.46	9.30	8.48	6.47	5.05	2.87	1.39
150	4.28	7.10	9.26	10.3	9.08	6.69	5.16	2.92	1.46
160	4.51	7.58	9.87	11.0	9.52	6.78	5.16	2.90	1.51
170	4.65	7.88	10.3	11.5	9.79	6.80	5.12	2.86	1.55
180	4.71	7.98	10.4	11.7	9.87	6.80	5.10	2.84	1.56

of Hall and Andrić,[22] Nishimura and Danjo,[23] and Khakoo et al.[24] In this figure, the two-state results of Schneider and Collins[17] and Baluja et al.,[18] obtained using the linear algebraic and R-matrix methods, respectively, are also shown. Our calculated cross sections and those of Schneider and Collins[17] and Baluja et al.[18] agree

well with the available experimental data[22–24] and with each other. The relatively small differences among these sets of calculated cross sections are probably due to the use of different basis sets and descriptions of target wave functions. However, there are significant differences between the results of these more recent two-state calculations and the earlier close-coupling results of Chung et al.[31] in which a restrictive orthogonality condition was imposed on the scattering function and target orbitals. The importance of such correlation terms in the scattering wave function could also be inferred from the two-state close-coupling studies of Weatherford in which the continuum orbital is either orthogonalized or left explicitly nonorthogonal to the occupied orbitals.[32] Finally, to provide some additional insight, in Table III we give the contributions of the $^2\Sigma_g$, $^2\Sigma_u$, $^2\Pi_u$, and $^2\Pi_g$ components of the scattering wave function to these excitation cross sections at eight energies.
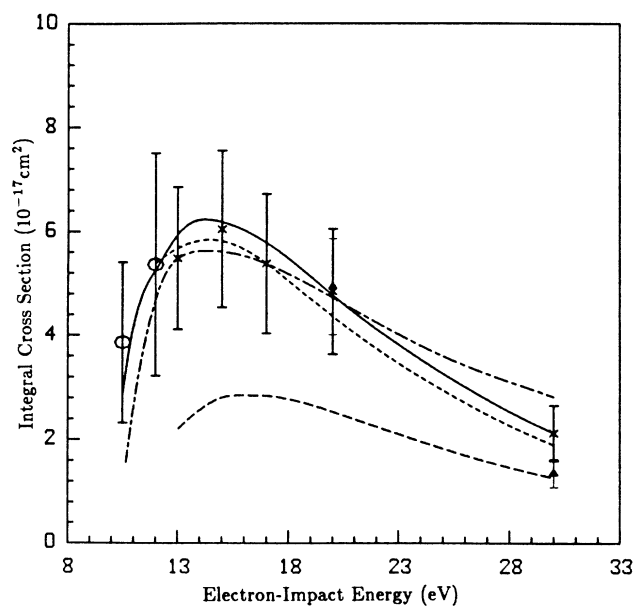

FIG. 7. Integral cross section for excitation of the $b\,^3\Sigma_u^+$ state: ———, present results; --- and —·—, calculated cross sections of Refs. 17 and 18, respectively; — — —, close-coupling results of Ref. 31; $\bigcirc$, $\times$, and $\blacktriangle$, measured values of Refs. 22, 23, and 24, respectively.

TABLE III. Symmetry contributions to the $X\,^1\Sigma_g^+ \to b\,^3\Sigma_u^+$ excitation cross sections $(10^{-17}\,cm^2)$.

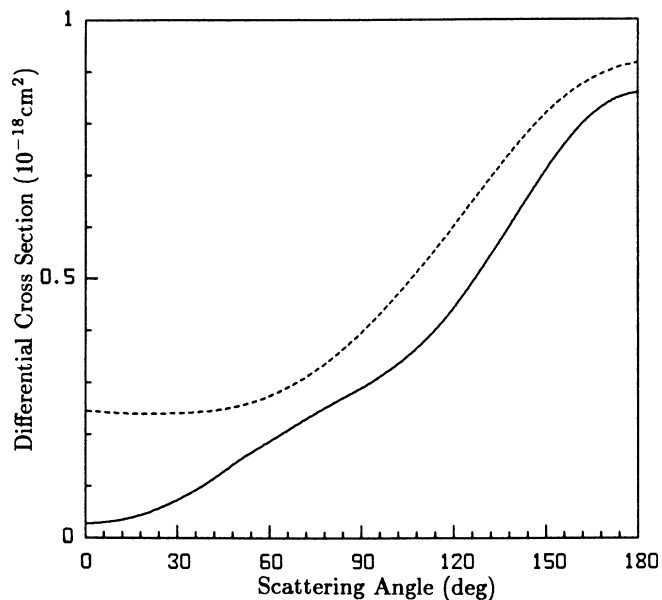| Energy (eV)	$^2\Sigma_g$	$^2\Sigma_u$	$^2\Pi_u$	$^2\Pi_G$	Total
10.5	0.21	2.48	0.0007	0.17	2.86
12	1.11	3.25	0.010	0.88	5.25
13	1.28	3.38	0.021	1.24	5.92
15	1.41	3.17	0.043	1.56	6.18
18	1.35	2.46	0.073	1.59	5.47
20	1.25	1.99	0.090	1.44	4.77
25	0.90	1.22	0.11	1.03	3.26
30	0.59	0.75	0.11	0.68	2.13

FIG. 8. Differential cross section for excitation of the $a\,^3\Sigma_g^+$ state at 13 eV: ———, present results; — — —, distorted-wave results of Ref. 33.
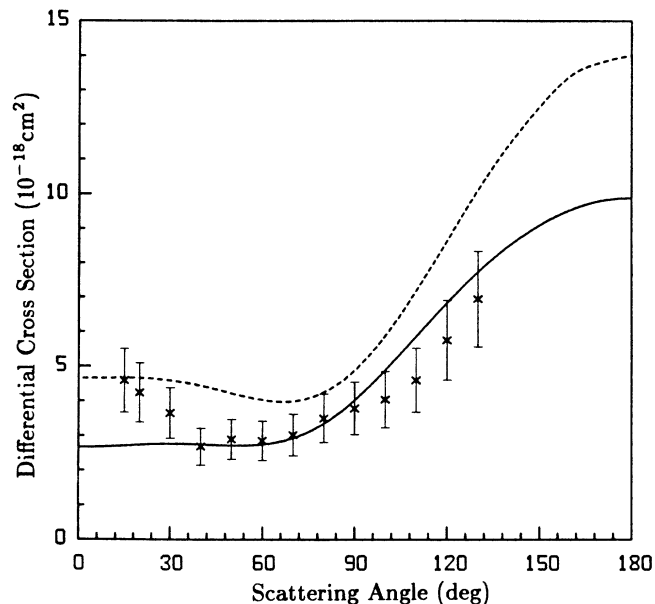

FIG. 10. Differential cross section for excitation of the $a\,^3\Sigma_g^+$ state at 20 eV: ———, present results; — — —, distorted-wave results of Ref. 33; ×, measured values of Ref. 34.

Calculated differential cross sections for excitation of $X\,^1\Sigma_g^+\rightarrow a\,^3\Sigma_g^+$ transition at 13, 14, 20, and 30 eV are shown in Figs. 8–11. These cross sections are again obtained including only the two open channels $X\,^1\Sigma_g^+$ and $a\,^3\Sigma_g^+$ and contributions from $^2\Sigma_g$, $^2\Sigma_u$, $^2\Pi_u$, and $^2\Pi_g$ overall symmetries in the expansion of the total scatter-

ing wave function. The differential cross sections for this excitation at several energies are shown in Table IV. At the lower energies, e.g., at 13 and 14 eV, no measured differential excitation cross sections are available. At these energies our two-state differential cross sections are generally similar to the distorted-wave results of Rescig-
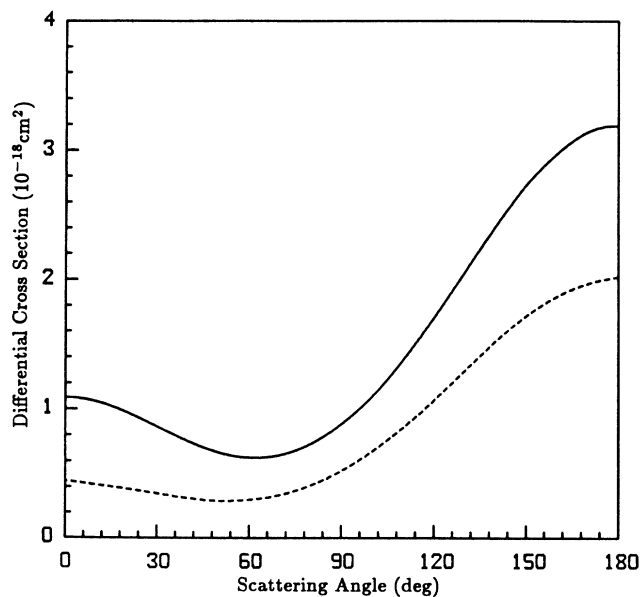

FIG. 9. Differential cross section for excitation of the $a\,^3\Sigma_g^+$ state at 14 eV: ———, present results; — — —, distorted-wave results of Ref. 33.
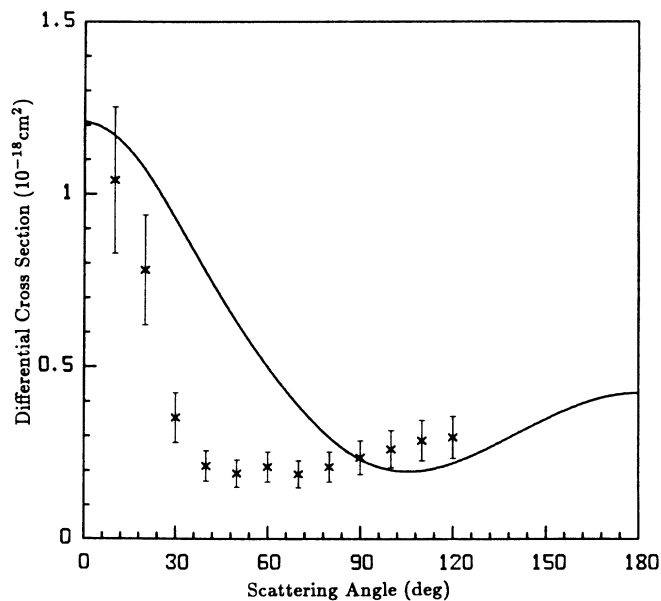

FIG. 11. Differential cross section for excitation of the $a\,^3\Sigma_g^+$ state at 30 eV: ———, present results; ×, measured values of Ref. 34.

TABLE IV. Differential cross sections for the $X\,{}^1\Sigma_g^+ \to a\,{}^3\Sigma_g^+$ excitation ($10^{-18}\mathrm{cm}^2/\mathrm{sr}$). The threshold energy is 12.036 eV.

Scattering angle (deg.)	Collision energy (eV)								
	12.5	13	14	15	16	18	20	25	30
0	0.011	0.028	1.09	2.43	2.86	2.97	2.77	1.79	1.21
10	0.013	0.033	1.06	2.35	2.78	2.88	2.68	1.73	1.17
20	0.018	0.048	0.977	2.15	2.54	2.62	2.43	1.57	1.07
30	0.025	0.074	0.866	1.85	2.19	2.25	2.09	1.34	0.926
40	0.035	0.107	0.754	1.53	1.81	1.84	1.71	1.10	0.773
50	0.045	0.146	0.667	1.23	1.44	1.45	1.35	0.883	0.628
60	0.055	0.186	0.627	1.00	1.14	1.12	1.04	0.695	0.498
70	0.062	0.223	0.647	0.863	0.922	0.855	0.792	0.540	0.387
80	0.068	0.257	0.732	0.824	0.796	0.670	0.605	0.418	0.296
90	0.072	0.289	0.885	0.875	0.758	0.565	0.482	0.330	0.233
100	0.077	0.327	1.10	1.01	0.800	0.543	0.429	0.284	0.202
110	0.085	0.377	1.38	1.20	0.914	0.603	0.453	0.285	0.200
120	0.097	0.444	1.71	1.44	1.08	0.739	0.553	0.335	0.222
130	0.113	0.528	2.06	1.70	1.29	0.937	0.719	0.428	0.259
140	0.132	0.620	2.41	1.96	1.52	1.17	0.928	0.549	0.304
150	0.151	0.710	2.73	2.19	1.73	1.40	1.15	0.677	0.349
160	0.168	0.787	2.97	2.38	1.91	1.60	1.34	0.790	0.388
170	0.180	0.838	3.14	2.50	2.02	1.74	1.47	0.868	0.415
180	0.184	0.856	3.19	2.54	2.06	1.78	1.52	0.895	0.425

no et al.,[33] which are also shown in Figs. 8 and 9. At 20 and 30 eV the present results are compared with the recent measurements of Khakoo and Trajmar[34] in Figs. 10 and 11. The agreement between the calculated and measured differential cross sections at 20 eV is excellent. The distorted-wave cross sections[33] are also qualitatively similar to these two-state results at this energy. There are, however, significant differences between our calculated and measured cross sections at 30 eV, particularly between 30° and 80°. Possible reasons for these differences are being studied.

Our calculated integral excitation cross sections for the $X\,{}^1\Sigma_g^+ \to a\,{}^3\Sigma_g^+$ transition are shown in Fig. 12 along with the two-state close-coupling results of Chung et al.,[31] Born-Rudge cross sections,[6] the distorted-wave results of Rescigno et al.,[33] and the experimental cross section of Khakoo and Trajmar[34] and of Ajello et al.[35] The cross sections of Khakoo and Trajmar[34] are from beam measurements, while those of Ajello et al.[35] are relative cross sections derived from optical-emission data. In Fig. 12 we have normalized the relative cross sections of Ajello et al.[35] to our calculated cross sections at 20 eV. The agreement between the present two-state results and the experimental data[34,35] is satisfactory. Both the calculated cross section and the data of Ajello et al.[35] show a rapid increase with energy just above threshold energy. In Table V we give the contributions by symmetry to these
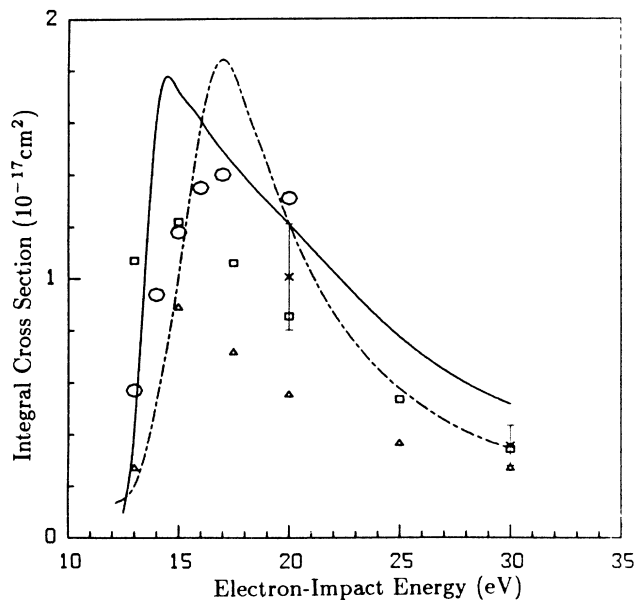

FIG. 12. Integral cross section for excitation of the $a\,{}^3\Sigma_g^+$ state; ——, present results; ○, distorted-wave results of Ref. 33; △, close-coupling values of Ref. 31; □, Born-Rudge results of Ref. 6; ×, measured values from beam measurements of Ref. 34; —·—, measured values derived from optical-emission data (Ref. 35). These values are normalized to our calculated cross sections at 20 eV.

TABLE V. Symmetry contributions to the $X\,{}^1\Sigma_g^+ \to a\,{}^3\Sigma_g^+$ excitation cross sections ($10^{-17}\,\mathrm{cm}^2$).

Energy (eV)	${}^2\Sigma_g$	${}^2\Sigma_u$	${}^2\Pi_u$	${}^2\Pi_g$	Total
13	0.21	0.19	0.000 58	0.016	0.42
14	0.38	1.21	0.000 44	0.017	1.61
15	0.50	1.21	0.000 88	0.018	1.73
16	0.63	0.93	0.001 3	0.030	1.59
18	0.60	0.69	0.052	0.049	1.39
20	0.53	0.55	0.081	0.045	1.21
25	0.31	0.33	0.11	0.018	0.77
30	0.19	0.21	0.11	0.0052	0.52

TABLE VI. Differential cross sections for the $X\,^1\Sigma_g^+\to c\,^3\Pi_u$ excitation ($10^{-18}\,\mathrm{cm^2/sr}$). The threshold energy is 12.306 eV.

Scattering angle (deg.)	Collision energy (eV)						
	13	15	16	18	20	25	30
0	2.29	11.3	12.5	12.8	12.0	8.03	4.16
10	2.24	11.1	12.3	12.6	11.8	7.85	4.11
20	2.09	10.6	11.9	12.0	11.1	7.31	3.92
30	1.90	9.71	11.1	11.1	9.97	6.45	3.54
40	1.71	8.65	9.93	9.72	8.54	5.34	2.98
50	1.58	7.48	8.59	8.16	6.98	4.14	2.31
60	1.54	6.34	7.18	6.58	5.47	3.05	1.65
70	1.63	5.36	5.87	5.18	4.20	2.21	1.13
80	1.86	4.67	4.84	4.11	3.27	1.67	0.783
90	2.22	4.40	4.26	3.48	2.71	1.40	0.601
100	2.72	4.62	4.19	3.28	2.49	1.33	0.547
110	3.32	5.31	4.58	3.47	2.55	1.39	0.576
120	3.99	6.38	5.32	3.93	2.84	1.51	0.642
130	4.71	7.67	6.22	4.55	3.28	1.65	0.708
140	5.41	9.03	7.12	5.23	3.82	1.77	0.745
150	6.05	10.3	7.94	5.90	4.40	1.85	0.744
160	6.58	11.4	8.58	6.48	4.93	1.87	0.714
170	6.92	12.1	9.00	6.88	5.32	1.85	0.679
180	7.04	12.4	9.15	7.03	5.46	1.84	0.664

integral cross sections. These values show that the $^2\Sigma$ components of the cross sections are dominant and that the sharp increase above threshold comes primarily from the $^2\Sigma_u$ channel. The significant differences between our two-state cross sections and the two-state close-coupling results of Chung et al.[31] are probably due to the absence of correlation terms in their wave function. Such terms relax the orthogonality condition imposed on the scattering and target orbitals.

Finally, we present cross sections for excitation of the $c\,^3\Pi_u$ state of H_2. We have carried out these calculations in two ways, using only one component of the degenerate $c\,^3\Pi_u$ state and using both the $^3\Pi_{ux}$ and $^3\Pi_{uy}$ components. The latter corresponds to a three-state calculation. We found no significant differences between these two- and three-state results. For example, the largest change in the integral cross sections was a reduction of about 6% in the two-state values going from a two- to three-state calculation. These reductions occurred primarily in the $^2\Sigma_g$ symmetry where the largest change was $0.08\times10^{-17}\,\mathrm{cm^2}$. We will see, furthermore, that contri-

butions from this symmetry are generally less than 10% of the total cross section. The cross sections shown in Tables VI and VII and Figs. 13–15 were obtained from a two-channel calculation with only the $X\,^1\Sigma_g^+$ and $c\,^3\Pi_{ux}$ states as open channels.

Figures 13 and 14 show our calculated differential cross section for excitation of the $c\,^3\Pi_u$ state at 20 and 30 eV, respectively, along with the experimental data of Khakoo and Trajmar.[34] Although the shapes of these calculated and measured cross sections, particularly those at 20 eV, are similar, there are substantial differences in their magnitudes. Differential cross sections at these and several other impact energies are again given in Table VI. In Fig. 15 we show our integral cross sections along with the distorted-wave results of Lee et al.,[36] Born-Rudge results of Chung et al.,[6] the close-coupling cross sections of Chung et al.,[31] and the data of Khakoo and Trajmar.[34] The agreement between our calculated cross sections and the measured values is again not good. Multichannel studies of these cross sections are clearly needed. The differences between our two-state results and

TABLE VII. Symmetry contributions to the $X\,^1\Sigma_g^+\to c\,^3\Pi_u$ excitation cross sections ($10^{-17}\,\mathrm{cm^2}$).

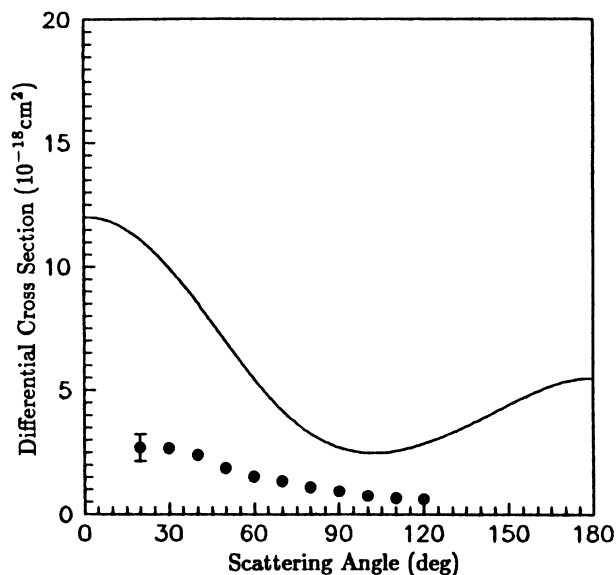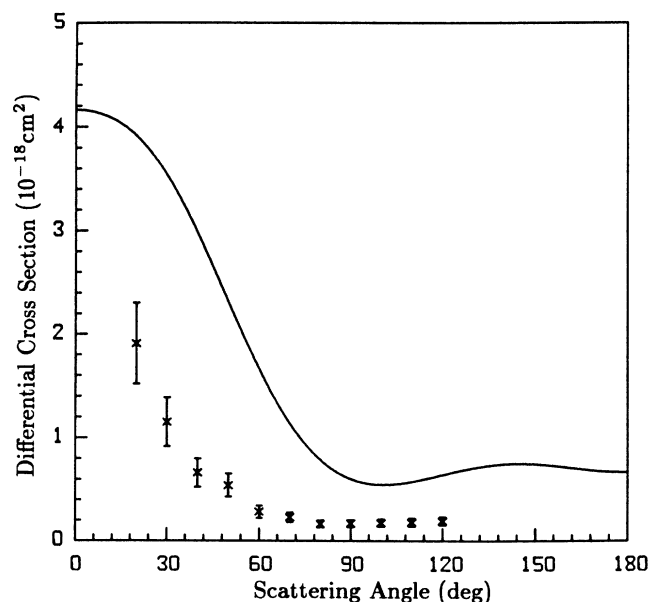| Energy (eV)	$^2\Sigma_g$	$^2\Sigma_u$	$^2\Pi_u$	$^2\Pi_g$	$^2\Delta_u$	$^2\Delta_g$	Total
13	0.20	0.0001	1.22	1.54	0.0021	0.80	3.76
15	0.51	0.0041	1.98	4.02	0.024	2.19	8.73
16	0.57	0.0080	2.18	3.51	0.037	2.10	8.41
18	0.67	0.015	1.83	2.60	0.061	2.05	7.23
20	0.62	0.020	1.41	1.86	0.075	1.91	5.90
25	0.39	0.031	0.79	0.74	0.095	1.22	3.27
30	0.23	0.030	0.35	0.33	0.083	0.59	1.61

FIG. 13. Differential cross section for excitation of the $c\,^3\Pi_u$ state at 20 eV: ——, present results; ●, measured values of Ref. 34.
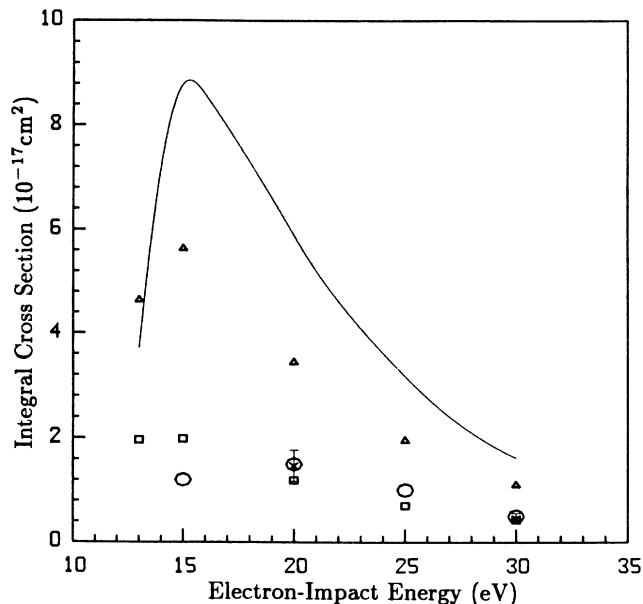

FIG. 15. Integral cross section for excitation of the $c\,^3\Pi_u$ state: ——, present results; △, close-coupling results of Ref. 31; ○, distorted-wave results of Ref. 36; □, Born-Rudge values of Ref. 6; ×, measured values of Ref. 34.

those of Chung et al.[31] are again probably due to the restrictive orthogonality conditions imposed on the scattering functions in their studies. Table VII gives the symmetry contributions to these integral cross sections. These values show that the $^2\Pi_u$, $^2\Pi_g$, and $^2\Delta_g$ contributions account for most of the excitation cross section.

FIG. 14. Differential cross section for excitation of the $c\,^3\Pi_u$ state at 30 eV: ——, present results; ×, measured values of Ref. 34.

IV. CONCLUSIONS

One of the objectives of this work was to use the Schwinger multichannel formulation[20,21] to study the low-energy electron-impact excitation cross sections for the $b\,^3\Sigma_u^+$, $a\,^3\Sigma_g^+$, and $c\,^3\Pi_u$ states of H_2 at the two-state level. These results, obtained for energies near threshold to 30 eV, could begin to provide much needed insight into the quantitative utility of such two-state studies of cross sections for electron-impact excitation of molecules at these energies. These studies show that, while the calculated cross sections for the $b\,^3\Sigma_u^+$ and $a\,^3\Sigma_g^+$ states agree quite well with available experimental data, those of the $c\,^3\Pi_u$ state differ significantly from the measured values at the two energies, 20 and 30 eV, where data is available. Multichannel studies of these excitation cross sections, designed to provide insight into the reasons for these and other differences between the two-state cross sections and the experimental data are under way.

*Present address: Instituto de Estudos Avancados, Centro Técnico Aeroespacial, Ministério de Aeronáutica, Caixa Postal 6044, 12 231 São José dos Campos, São Paulo, Brazil.

†Present address: Department of Physics, Texas Tech University, Lubbock, Texas 79409.

[1]See, for example, Swarm Studies and Inelastic Electron-Molecule Collisions: Proceedings of the Meeting of the Fourth International Swarm Seminar and the Inelastic Electron-Molecule Collisions Symposium, edited by L. Pitchford, V. McKoy, A. Chutjian, and S. Trajmar (Springer-Verlag, New York, 1986).

[2]See, for example, S. C. Brown, Electron-Molecule Scattering (Wiley, New York, 1979).

[3]C. Park, J. Spacecr. Rockets 22, 27 (1985).

[4]Ph. Avouris and J. E. Demuth, Ann. Rev. Phys. Chem. 34, 49 (1984).

[5]See, for example, S. Trajmar, D. F. Register, and A. Chutjian, Phys. Rep. 97, 219 (1983). For a short review of recent theoretical progress in the theory of electron-impact excitation of molecules see the article by L. A. Collins and B. I. Schneider, in Electronic and Atomic Collisions, edited by H. B. Gilbody, W. R. Newell, F. H. Read, and A. C. H. Smith (Elsevier, Amsterdam, 1988).

[6]S. Chung, C. C. Lin, and E. T. P. Lee, Phys. Rev. A 12, 1340 (1975).

[7]D. C. Cartwright and A. Kuppermann, Phys. Rev. 163, 86 (1967).

[8]A. U. Hazi, Phys. Rev. A 23, 2232 (1981).

[9]T. N. Rescigno, C. W. McCurdy, Jr., and V. McKoy, J. Phys. B 7, 2396 (1974).

[10]A. W. Fliflet and V. McKoy, Phys. Rev. A 21, 1863 (1980).

[11]M.-T. Lee and V. McKoy, Phys. Rev. A 28, 697 (1983).

[12]See, for example, Electron-Atom and Electron-Molecule Collisions, edited by J. Hinze (Plenum, New York, 1983); L. A. Collins and B. I. Schneider, Phys. Rev. A 24, 2387 (1981).

[13]J. Tennyson, C. J. Noble, and S. Salvini, J. Phys. B 17, 905 (1984).

[14]J. Tennyson and C. J. Noble, J. Phys. B 18, 155 (1985).

[15]B. I. Schneider and L. A. Collins, Phys. Rev. A 33, 2982 (1986).

[16]M. A. P. Lima, T. L. Gibson, W. M. Huo, and V. McKoy, J. Phys. B 18, L865 (1985).

[17]B. I. Schneider and L. A. Collins, J. Phys. B 18, L857 (1985).

[18]K. L. Baluja, C. J. Noble, and J. Tennyson, J. Phys. B 18, L851 (1985).

[19]C. J. Noble and P. J. Burke, J. Phys. B 19, L19 (1986).

[20]K. Takasuka and V. McKoy, Phys. Rev. A 24, 2473 (1981).

[21]K. Takatsuka and V. McKoy, Phys. Rev. A 30, 1734 (1984).

[22]R. I. Hall and L. Andrić, J. Phys. B 17, 3815 (1984).

[23]H. Nishimura (private communication). The results shown here are essentially equivalent to those published by H. Nishimura and A. Danjo, J. Phys. Soc. Jpn. 55, 3031 (1986) except below 50° at 13 eV. At these points the published cross sections are smaller than the experimental values shown in Fig. 3.

[24]M. A. Khakoo, S. Trajmar, R. McAdams, and T. W. Shyn, Phys. Rev. A 35, 2832 (1987).

[25]M. A. P. Lima, T. L. Gibson, K. Takatsuka, and V. McKoy, Phys. Rev. A 30, 1741 (1984).

[26]T. L. Gibson, M. A. P. Lima, V. McKoy, and W. M. Huo, Phys. Rev. A 35, 2473 (1987).

[27]M. A. P. Lima and V. McKoy, Phys. Rev. A 38, 501 (1988).

[28]See, for example, D. K. Watson and V. McKoy, Phys. Rev. A 20, 1474.

[29]W. M. Huo, T. L. Gibson, M. A. P. Lima, and V. McKoy, Phys. Rev. A 36, 1632 (1987).

[30]W. A. Goddard III and W. J. Hunt, Chem. Phys. Lett. 24, 464 (1974).

[31]S. Chung and C. C. Lin, Phys. Rev. A 17, 1874 (1978); T. K. Holley, S. Chung, C. C. Lin, and E. T. P. Lee, ibid. 26, 1852 (1982).

[32]C. A. Weatherford, Phys. Rev. A 22, 2519 (1980).

[33]T. N. Rescigno, C. W. McCurdy, Jr., V. McKoy, and C. F. Bender, Phys. Rev. A 13, 216 (1976).

[34]M. A. Khakoo and S. Trajmar, Phys. Rev. A 34, 146 (1986).

[35]J. M. Ajello, K. D. Pang, B. Franklin, and F. Flam, Abstracts of the American Geophysical Union Fall Meeting, San Francisco, 1985 [Eos Trans. Am. Geophys. Union 66, 989 (1985)].

[36]M. T. Lee, R. R. Lucchese, and V. McKoy, Phys. Rev. A 26, 3240 (1982).